previously reported the Zeeman effect on the $^6P_{7/2}$ fluorescence of CaF_2:Gd^{3+} at cubic sites. Their results are in agreement with the work described here.

ACKNOWLEDGMENTS

The author is deeply indebted to V. L. Donlan and Dr. J. M. O'Hare for sharing their results prior to publication and for many helpful discussions. I would also like to thank Dr. P. P. Yaney for suggesting this problem for the x-ray analysis and for stimulating discussions, and J. C. Rawers for assistance in taking the data. The use of laboratory facilities of the Air Force Materials Laboratory (W-PAFB) is gratefully acknowledged. Figure 2 and Table V are reproduced from Ref. 5 with the generous permission of the North-Holland Publishing Co.

PHYSICAL REVIEW VOLUME 185, NUMBER 2 10 SEPTEMBER 1969

Linewidths and Thermal Shifts of Spectral Lines in Neodymium-Doped Yttrium Aluminum Garnet and Calcium Fluorophosphate

TAKASHI KUSHIDA
Bell Telephone Laboratories, Murray Hill, New Jersey 07974
(Received 10 March 1969)

Measurements in the 4.2–500°K temperature range are reported of the widths, shapes, and thermal shifts of the 1.06- and 0.9-μ lines of the Nd^{3+} ions in yttrium aluminum garnet (YAlG) and calcium fluorophosphate. The results are interpreted in terms of phonon-impurity interactions and static crystal strains. The obtained effective Debye temperature of YAlG is compared with the phonon density spectrum deduced from vibronic sidebands of the R lines in YAlG:Cr^{3+}. The $R \rightarrow Z_5$ and $R \rightarrow Y_6$ transitions of YAlG:Nd are observed to shift exceptionally to the higher energies with an increase of temperature. This is tentatively ascribed to the pushing effect of nearby higher-lying manifolds. Comparison of widths of several lines in YAlG:Nd at low temperatures reveals that the fluctuation of the second-degree crystal-field parameters contributes to the inhomogeneous linebroadenings. Discussions are also presented on the suitability of hard crystals with high phonon cutoff frequencies for the laser host materials.

I. INTRODUCTION

SUCCESS of solid-state lasers has stimulated studies on sharp optical transitions of impurity ions in crystals, and several factors which determine the widths, positions, and shapes of these spectral lines have been clarified by a number of investigators. In addition to static crystal strains and impurity-impurity interaction, phonon-impurity interaction makes an important contribution, and the thermal behaviors of linewidths and line positions are mostly explained in terms of this interaction. Recent studies in several narrow lines of $3d$ and $4f$ ions in crystals have revealed that the direct (one-phonon) process and the Raman (two-phonon) process play predominant roles in homogeneous broadenings and thermal shifts of these lines.[1–4] In a laser line, the linwidth and thermal shift have significant meaning, since these properties are closely related to the light amplification gain, output frequency stability, and thermal tunability of the laser.

In the present paper, measurements are reported of the widths, shapes, and thermal shifts of several lines of the Nd^{3+} ions in yttrium aluminum garnet (YAlG) and calcium fluorophosphate (FAP) in the 4.2–500°K temperature range. Experimental data are well explained by static crystal strains and phonon-impurity interactions. The temperature dependences of the positions and linewidths are in reasonable agreement with existing theory, which assumes a Debye model for the phonons. YAlG:Nd and FAP:Nd are very useful laser materials with low threshold and high efficiency.[5,6] This excellence may be related in part to the narrow spectral widths of the laser lines and further to the phonon-impurity interactions in these materials.

II. REVIEW OF THEORY AND RELATED EXPERIMENTS

The crystalline field at the impurity ion is a function of the local strain ϵ. Spatially nonuniform crystal strains give rise to inhomogeneous spectral linebroadening and strains due to externally applied pressure produce stress-induced line shifts. When ϵ is a dynamic strain due to the lattice vibrations, the inter-

[1] D. E. McCumber and M. D. Sturge, J. Appl. Phys. **34**, 1682 (1963).
[2] G. F. Imbusch, W. M. Yen, A. L. Schawlow, D. E. McCumber, and M. D. Sturge, Phys. Rev. **133**, A1029 (1964).
[3] W. M. Yen, W. C. Scott, and A. L. Schawlow, Phys. Rev. **136**, A271 (1964).
[4] T. Kushida and M. Kikuchi, J. Phys. Soc. Japan **23**, 1333 (1967).
[5] J. E. Geusic, H. M. Marcos, and L. G. Van Uitert, Appl. Phys. Letters **4**, 182 (1964).
[6] R. C. Ohlmann, K. B. Steinbruegge, and R. Mazelsky, Appl. Opt. **7**, 905 (1968).

action between the impurity and the local crystalline field causes temperature-dependent broadenings and shifts of the energy levels of the ion. To understand these thermal behaviors, usually a simplified impurity-phonon interaction,

$$H_I = C\epsilon + D\epsilon^2 = H^{(1)} + H^{(2)}, \tag{1}$$

is adopted, where C and D are linear and quadratic coupling parameters.[1-4] With this Hamiltonian and a Debye distribution of phonons having a characteristic temperature Θ_D, the width of an impurity level $|1\rangle$ may be written as

$$\Gamma_1(T) = \Gamma_1'(0) + \Gamma_1^D(T) + \Gamma_1^R(T), \tag{2}$$

$$\Gamma_1^D(T) = \frac{1}{2\pi\rho_m v^5}\left[\sum_{j>1} |C_{1j}|^2 \omega_{j1}^3 n(\omega_{j1}) + \sum_{j<1} |C_{1j}|^2 \omega_{1j}^3 \{n(\omega_{1j})+1\}\right],$$

$$\Gamma_1^R(T) = \frac{(a+a')(kT)^7}{2\pi^3\rho_m^2\hbar^6 v^{10}} \int_0^{\Theta_D/T} \frac{x^6 e^x}{(e^x-1)^2} dx = \bar{\alpha}_1 \left(\frac{T}{\Theta_D}\right)^7 \xi_6\left(\frac{\Theta_D}{T}\right),$$

with

$$a = \left(D_{11} + \sum_{j\neq 1} \frac{|C_{1j}|^2}{E_1 - E_j}\right)^2,$$

$$a' = \sum_{j\neq 1} \left| D_{1j} + \sum_{i(\neq 1,j)} \frac{C_{1i}C_{ij}}{2}\left(\frac{1}{E_1-E_j} + \frac{1}{E_j-E_i}\right)\right|^2,$$

and

$$\xi_6(Z) = \int_0^Z \frac{x^6 e^x}{(e^x-1)^2} dx.$$

Here, ρ_m and v are the mass density and the average sound velocity of the crystal, and $n(\omega_{ij}) = [\exp(\hbar\omega_{ij}/kT)-1]^{-1}$ is the occupation number of the phonons with energy $\hbar\omega_{ij} = E_i - E_j (\lesssim k\Theta_D)$. C_{ij} and D_{ij} are the matrix elements of the coupling operators C and D between the impurity levels $|i\rangle$ and $|j\rangle$. Statistical strain broadenings and other mechanisms which are assumed to be temperature insensitive are included in $\Gamma_1'(0)$. While $\Gamma_1^D(T)$ results from the absorption or emission of a single resonant phonon, $\Gamma_1^R(T)$ represents the contribution of two-phonon Raman scattering.

Similarly, the energy of an impurity level may be expressed as

$$E_1(T) = E_1(0) + E_1^D(T) + E_1^R(T),$$

$$E_1^D(T) = \sum_{j\neq 1} |C_{ij}|^2 \frac{(E_j-E_1)(KT)^2}{2\pi^2\rho_m v^5\hbar^3} P\int_0^{\Theta_D/T} \frac{x^3}{e^x-1} \times \frac{1}{x^2 - [(E_j-E_1)/kT]^2} dx, \tag{3}$$

$$E_1^R(T) = \left[D_{11} + \sum_{j\neq 1} \frac{|C_{1j}|^2}{E_1-E_j}\right] \frac{(kT)^4}{2\pi^2\rho_m v^5\hbar^3} \times \int_0^{\Theta_D/T} \frac{x^3}{e^x-1} dx = \alpha_1 \left(\frac{T}{\Theta_D}\right)^4 \int_0^{\Theta_D/T} \frac{x^3}{e^x-1} dx,$$

where P denotes the principal value of the integral.[7] The homogeneous width of a spectral line is given by the sum of the homogeneous widths of the two relevant energy levels, while the transition energy or spectral line position is given by the difference of the two relevant level energies.[8]

Usually the above equations considering only the direct and Raman processes explicitly are employed to fit experimental data, where the coupling parameters and effective Debye temperature Θ_D are treated as adjustable parameters. Moderate fits over a wide temperature range have been reported for several lines of $3d$, $4f$, and $5f$ ions.[1-4,9] Further, reasonable agreement was obtained by a nonempirical calculation of the absolute values of linewidths and pressure-induced changes of the splittings for the R, R', and B absorption lines in ruby.[4,10] Although actual phonon spectra of crystals are complicated and are often far from the Debye model, the integration process smears out bumps in the spectra and the thermal behavior is usually well described by a single characteristic temperature. This temperature does not always coincide with the Debye temperature determined from specific-heat data, because all the phonons are not coupled to the metal ion effectively. Sometimes a more realistic effective phonon-density spectrum is deduced from vibronic sidebands of no-phonon lines.[2-4]

Broadening mechanisms such as the Raman process which predicts an energy-independent damping factor give a perfectly Lorentzian line shape, while a Gaussian shape may be expected for statistical strain broadenings. The direct process causes asymmetric broadening because of the energy-dependent one-phonon relaxation rate.[4] Since different line shapes are expected for several broadening mechanisms, simple summation of Eq. (2)

[7] There seem to be some misprints in the literature. $(T_e/\Theta_D)^2$ of the denominator of the integrand in the expression for the direct-shift term of Refs. 1 and 3 should be $(T_e/T)^2$. The sign of the expression for energy shift in Refs. 3 and 8 should be reversed. This is because their definition for strain ϵ gives an imaginary value if we assume that a_k and a_k^+ are Hermitian conjugate. This fact was pointed out to the author by Dr. M. Kikuchi, to whom he is indebted.

[8] G. F. Imbusch, W. M. Yen, A. L. Schawlow, G. E. Devlin, and J. P. Remeika, Phys. Rev. **136**, A481 (1964).

[9] J. V. Nicholas, Phys. Rev. **155**, 151 (1967).

[10] A calculation of $E_1^R(T)$ similar to that of Ref. 4, using zeroth-order wave functions and only the $H^{(1)}$ term of Eq. (1), yields $\alpha_1 = -286$ cm^{-1} for the ^2E state and $\alpha_1 = -92$ cm^{-1} for the ground state of ruby. The difference, -194 cm^{-1}, should be compared with the experimentally determined Raman-shift coefficient of -400 cm^{-1} for the R_1 line (Ref. 1). The agreement is again very good in view of the approximations used.

is a rough approximation and it is necessary, to be accurate, to decompose a line into a few appropriate components.

When the crystal temperature is increased, energy levels and, therefore, spectral lines broaden invariably as the higher phonon states are occupied. Since there are many high-lying energy levels which couple, the $E_1^R(T)$ term normally lowers an energy level ($\alpha_1<0$). Further, it is usually the case that the dependence with temperature of higher levels is larger than for lower levels because of smaller energy denominators. As a result, the spectral lines are observed to shift normally to the longer wavelengths when the temperature is increased.[11] On account of the principal value of the integral, the effect of the $E_1^D(T)$ term is complicated. Generally speaking, when the energy separation is comparable to or bigger than the phonon cutoff energy of the crystal, two levels for which the matrix element of $H^{(1)}$ does not vanish repel each other by the effect of the $E_1^D(T)$ term. On the contrary, when the energy separation is small, this term tends to attract each level, except for the low-temperature region where the energy separation is much larger than kT. This effect seems to be observable in reported experimental data (for example, Fig. 16 of Ref. 3 and Fig. 2 of Ref. 11).

Thermal expansion of the crystal lattice causes changes of crystalline-field strength and accordingly changes of impurity-level energies. Paetzold[12] compared thermal shifts with pressure-induced shifts for several lines of Cr^{3+} and Nd^{3+}. Thermal shifts to the blue were observed over portions of the temperature range for some of the $Z \rightarrow E$ transitions of Nd^{3+} in the soft hydrated crystal $Pr(NO_3)_3 \cdot 6H_2O$. They are opposite to the red pressure shifts and are considered to be mainly due to the thermal changes of the lattice parameters. However, in hard crystals of ruby and alexandrite, thermal shifts and pressure shifts were always to the red, showing minor contribution of the crystal expansions. Johnson *et al.*'s observation[11] of red thermal shifts of the $Z \rightarrow E$ transitions in LaF_3:Nd gives a support to Paetzold's conjecture that the effect of thermal expansion is negligible in hard ionic crystals.

III. EXPERIMENTAL PROCEDURE

The specimens employed were 1–2 mm thick and contained 0.2–1 at.% of Nd^{3+} ions. A Jarrell-Ash 1-m Ebert scanning spectrometer with a 15 000-lines/in. grating blazed for 2 μ was used in the second order. The minimum spectral slit width employed corresponded to about 0.3 cm^{-1}. Luminescence was excited with a high-pressure Osram HBO 500-W mercury lamp through a Corning glass color filter CS4-97. A liquid-nitrogen cooled RCA 7102 photomultiplier was used to detect the signal. The temperature of the specimen was controlled by direct immersion in liquid coolants, by blowing nitrogen gas, and by use of an electric heater. Positions of narrow spectral lines were reproducible to ± 0.2 Å. Typical accuracy of the linewidth measurement was $\pm 10\%$.

IV. EXPERIMENTAL RESULTS AND INTERPRETATIONS

A. Fluorescence Spectrum

Flourescence spectra in the 0.9-μ and 1.06-μ wavelength region were measured between 4.2 and 500°K. The energies of the initial and final states of the observed spectral lines were determined at 77°K and are shown in Fig. 1. We shall use nomenclature for energy levels which is usually employed in the literature,[13] i.e., R, Y, and Z for the $^4F_{3/2}$, $^4I_{11/2}$, and $^4I_{9/2}$ manifolds,

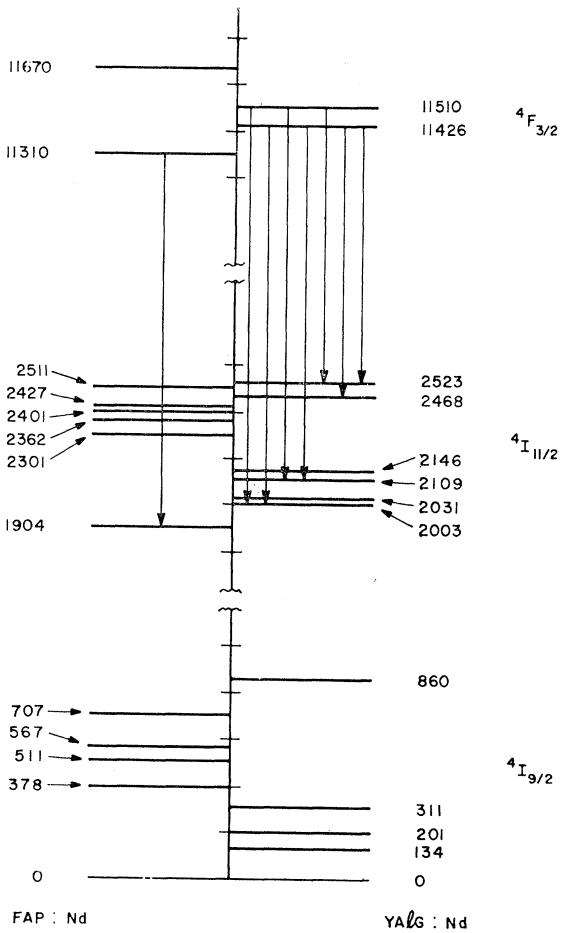

FIG. 1. Energy levels of three manifolds of Nd^{3+} in YAlG and FAP. The energies were determined at 77°K. The transitions on which laser oscillation has been reported are indicated by vertical arrows.

[11] S. A. Johnson, H. G. Freie, A. L. Schawlow, and W. M. Yen, J. Opt. Soc. Am. **57**, 734 (1967).
[12] H. K. Paetzold, Z. Physik **139**, 129 (1951).
[13] E. H. Carlson and G. H. Dieke, J. Chem. Phys. **34**, 1602 (1961).

respectively, and 1, 2, 3, ··· from the bottom for Stark levels within a manifold. At room temperature, YAlG:Nd and FAP:Nd lasers normally oscillate on the most intense lines at 1.064 μ ($R_2 \rightarrow Y_3$) and 1.063 μ ($R_1 \rightarrow Y_1$), respectively.[5,6] Recently, however, using a dispersive prism inside the cavity, Smith[14] succeeded in producing cw room-temperature oscillations on several other lines of YAlG:Nd. The transitions on which laser oscillation has been reported are shown by arrows in Fig. 1.

The shapes of most lines examined were nearly Lorentzian over a wide temperature range, though there were a few exceptions, such as the 0.899-μ ($R_1 \rightarrow Z_4$) line of YAlG:Nd, which was clearly asymmetric over the entire temperature region measured and had longer tails on the lower-energy side. At low temperatures, several lines showed deviation from the Lorentzian shape which indicates the existence of strain broadening components. The 1.06-μ laser line of YAlG:Nd that appears asymmetric at room temperature can be resolved into two Lorenzian lines corresponding to the $R_2 \rightarrow Y_3$ and $R_1 \rightarrow Y_2$ transitions.[15]

Besides several lines which were unambiguously assigned to the $R \rightarrow Y$ and Z transitions,[16] weak narrow lines were observed in YAlG:Nd at low temperatures in the same spectral region. These satellite lines were about two orders less intense than the main lines and this ratio did not change appreciably by the purification of the starting material. Some of these satellite lines had narrower widths than nearby main lines and the excitation spectra for satellites and main lines were very similar. These observations may suggest that these satellites result from Nd-Nd pairs or the Nd ions in other than Y^{3+} sites. In FAP:Nd, there were also several narrow satellite lines whose intensities were almost comparable to those of main lines.[6]

All the YAlG:Nd specimens examined showed red emissions around 0.7 μ due to the Cr^{3+} impurity. The spectrum coincided with reported data on YAlG:Cr.[17] In this case, the narrow R lines were accompanied by broad satellite bands, and the ratio of the peak intensity of the R lines to that of the Stokes sideband was about 4–6 to 1 at 77°K.

B. Thermal Shifts of Line Positions

Measurements were made of the temperature dependence of the positions of the spectral lines corresponding to the $R \rightarrow Y$ and $R \leftrightarrow Z$ transitions in the 4.2 to 500°K temperature range. Almost all lines shifted to the longer wavelengths with increasing temperature. Exceptions were the 0.94-μ ($R \rightarrow Z_5$) and 1.12-μ ($R \rightarrow Y_6$) emission lines of YAlG:Nd, which showed clear blue-shifts. Thermal shifts were very small for the $R \rightarrow Y_5$ transitions of YAlG:Nd and the $Z_1 \rightarrow R_2$, $R_1 \rightarrow Y_6$ transitions of the FAP:Nd. Typical experimental data are shown in Figs. 2 and 3. Rates of the

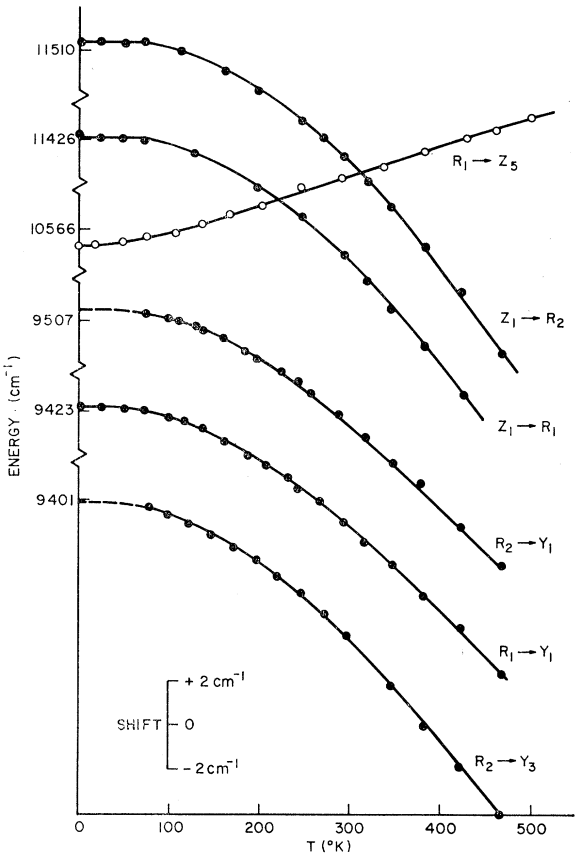

FIG. 2. Typical examples of temperature dependence of line positions in YAlG:Nd.

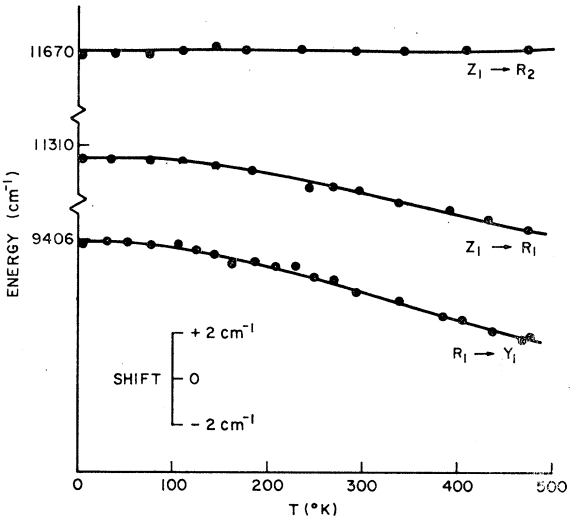

FIG. 3. Typical examples of temperature dependence of line positions in FAP:Nd.

[14] R. G. Smith, IEEE J. Quantum Electron. **QE-4**, 505 (1968).
[15] T. Kushida, H. M. Marcos, and J. E. Geusic, Phys. Rev. **167**, 289 (1968).
[16] J. A. Koningstein and J. E. Geusic, Phys. Rev. **136**, A711 (1964).
[17] G. Burns, E. A. Geiss, B. A. Jenkins, and M. I. Nathan, Phys. Rev. **139**, A1687 (1965).

thermal energy shifts of the laser lines were 0.04 and 0.01 cm^{-1}/deg at room temperature for the 1.064-μ line of YAlG:Nd and the 1.063-μ line of the FAP:Nd, respectively.

Thermal shifts were also examined for the absorption lines of YAlG:Nd in the 18 700–19 600-cm^{-1} energy region up to room temperature. These lines include the $Z \rightarrow E$ transitions of Nd^{3+}, for which studies of thermal and pressure shifts have been done in $Pr(NO_3)_3 \cdot 6H_2O$:Nd and LaF_3:Nd.[12,11] All the lines of YAlG:Nd in this region showed red-shifts as temperature was increased.

As shown in Fig. 4, observed energy shifts of the $R_1 \rightarrow Y_1$ transitions can be fitted well to the Raman-shift term of the theory with T_D of 600 and 500°K, respectively, for YAlG and FAP crystals. Moderate fits were also obtained for relatively large red thermal shifts of the $R \rightarrow Y_i$, $R \rightarrow Z_i$ ($i=1, 2, 3$, and 4) transitions of YAlG:Nd, though the effective Debye temperature thus determined differed slightly among these lines. This difference may be ascribed mainly to the contribution of $E_1^D(T)$ and other neglected terms. The origin of the observed blue shift is not simple and will be discussed in a later section.

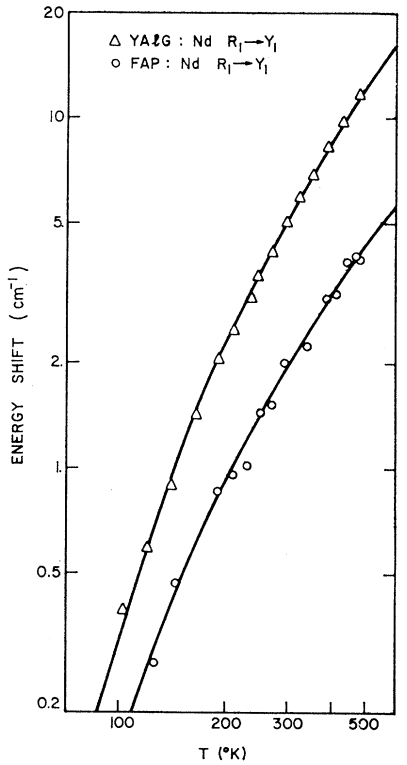

FIG. 4. Comparison with theory of energy shifts of the $R_1 \rightarrow Y_1$ transitions in YAlG-Nd and FAP:Nd. The theoretical curves are

$$E(T)-E(0)=\left[-73(T/600°\mathrm{K})^4\int_0^{600°\mathrm{K}/T}\frac{x^3}{e^x-1}dx\right] \mathrm{cm}^{-1}$$

for the 1.062-μ line of YAlG:Nd, and

$$E(T)-E(0)=\left[-19.5(T/500°\mathrm{K})^4\int_0^{500°\mathrm{K}/T}\frac{x^3}{e^x-1}dx\right] \mathrm{cm}^{-1}$$

for the 1.063-μ line of FAP:Nd.

The separation of the R states in YAlG:Nd was about 84 cm^{-1} and increased with temperature by a barely detectable amount. Since this separation is much smaller than the phonon cutoff energy of YAlG, the resonant phonon transitions between these states are expected to decrease the separation. Therefore, this result is interpreted to imply that the contribution of the $E_1^D(T)$ term due to the direct $R_2 \leftrightarrow R_1$ process is small compared with the difference of the magnitudes of the Raman terms between the two R states. On the other hand, the increase with temperature of the R-level splitting of FAP:Nd can be explained by repulsion of two R states via the direct interaction and/or by the difference of the Raman shift coefficients for these two states.

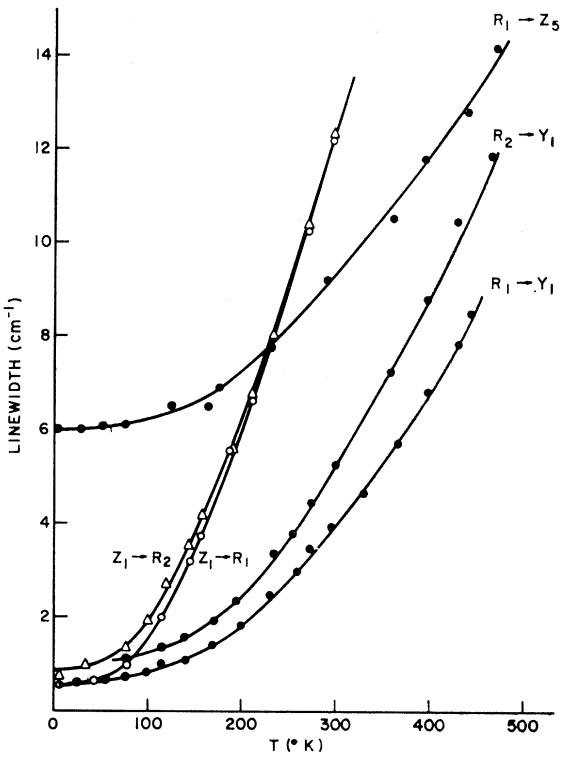

FIG. 5. Full widths at half-maximum of several lines of YAlG:Nd, as a function of temperature.

C. Temperature Dependence of Linewidths

Typical examples of measured thermal behaviors of spectral linewidths are shown in Figs. 5 and 6. In Fig. 7, experimental data for the $R \rightarrow Y_1$ transitions are compared with Eq. (2) in which we neglected the $\Gamma_1^D(T)$ term. For a good fit, we must assume different characteristic temperatures from those for the thermal

line shifts. This is not very surprising, because the phonon spectra of these crystals are considered to be complicated and very different from the Debye spectrum. Since the lines of FAP:Nd have broad residual widths at very low temperatures and since there is ambiguity in the simple additive form of Eq. (2), Θ_D of 900°K for FAP may be somewhat overestimated.

Although is was possible to fit all the linewidth data to Eq. (2), too many unknown parameters prevented an accurate determination of the relative contributions of the strain, direct, and Raman processes. For example, the temperature dependence of the $R_1 \rightarrow Z_5$ linewidth

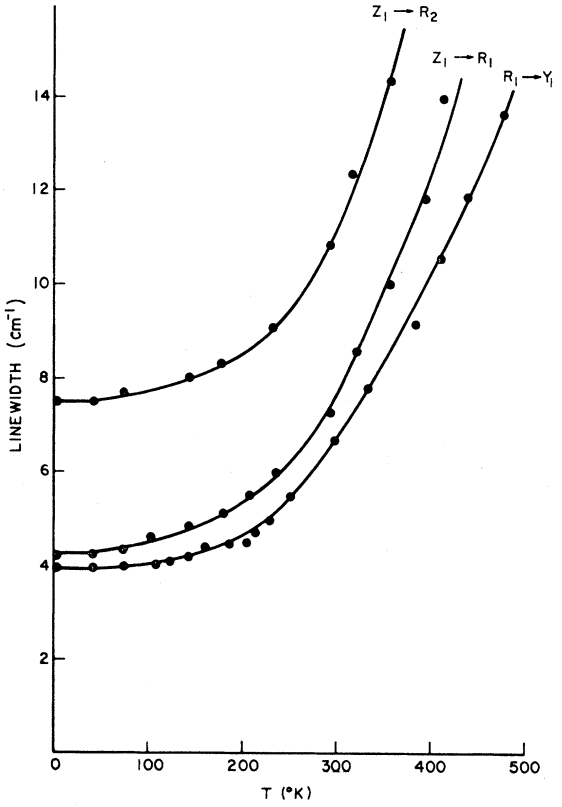

FIG. 6. Full widths at half-maximum of three lines of FAP:Nd as a function of temperature.

of YAlG:Nd agrees with both

$$\Gamma(T)=[6+50(T/\Theta_D)^7\xi_6(\Theta_D/T)]\ \text{cm}^{-1}$$

and

$$\Gamma(T)=[6(n+1)+42(T/\Theta_D)^7\xi_6(T/\Theta_D)^7]\ \text{cm}^{-1},$$

where $\Theta_D=500$°K, and $n=[\exp(549\ \text{cm}^{-1}/kT)-1]^{-1}$. In this case, however, the relatively large residual width appears to be mainly due to the direct $Z_5 \rightarrow Z_4$, Z_3, $\cdots$ processes, because this line is almost Lorentzian even at 4.2°K. It is difficult to explain the thermal behavior of the $Z_1 \rightarrow R_1$, R_2 linewidths of YAlG:Nd without the $\Gamma_1^D(T)$ term. The direct phonon absorptions are considered to play important roles in the broadening

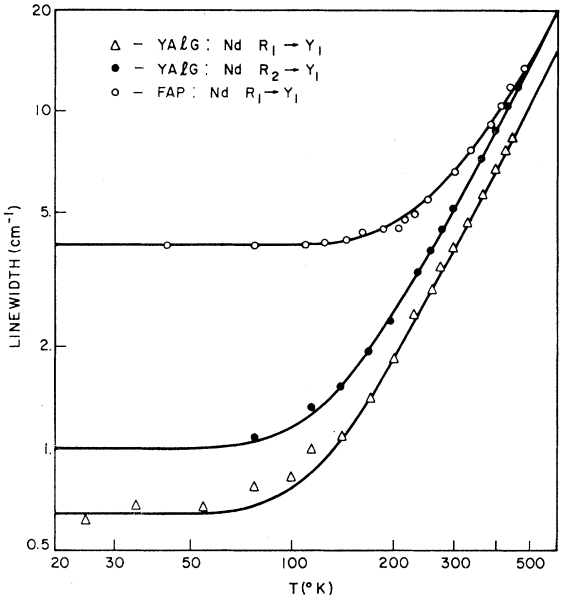

FIG. 7. Comparison with theory of thermal broadenings of the $R \rightarrow Y_1$ transitions in YAlG:Yd and FAP:Nd. The theoretical curves are

$$\Gamma(T)=[0.64+53(T/500\text{°K})^7\xi_6(500\text{°K}/T)]\ \text{cm}^{-1}$$

for the $R_1 \rightarrow Y_1$ transition in YAlG:Nd,

$$\Gamma(T)=[1.0+68(T/500\text{°K})^7\xi_6(500\text{°K}/T)]\ \text{cm}^{-1}$$

for the $R_2 \rightarrow Y_1$ transition in YAlG:Nd, and

$$\Gamma(T)=[4.0+200(T/900\text{°K})^7\xi_6(900\text{°K}/T)]\ \text{cm}^{-1}$$

for the $R_1 \rightarrow Y_1$ transition is FAP:Nd.

of the ground state. By fitting the linewidth data to Eq. (2), it was concluded that the $Z_1 \rightarrow Z_2$ and Z_3 processes are especially important. The experimental observation that the residual widths of the transitions from the R_1 level to the $Z_2(\sim 7\ \text{cm}^{-1})$, $Z_3(\sim 5\ \text{cm}^{-1})$, $Z_4(\sim 16\ \text{cm}^{-1})$, $Z_5(\sim 6\ \text{cm}^{-1})$, $Y_4(\sim 3\ \text{cm}^{-1})$, $Y_5(\sim 9\ \text{cm}^{-1})$, and $Y_6(\sim 8\ \text{cm}^{-1})$ levels are much broader than those of the other $R_1 \rightarrow Y$ and $R_1 \rightarrow Z_1$ transitions ($\lesssim 1\ \text{cm}^{-1}$) in YAlG:Nd may show relatively large effects of the direct processes on the line broadenings. Since there are several possible direct processes, such as $Z_4 \rightarrow Z_1$, Z_2, Z_3, and Z_5 transitions, and since the inhomogeneous widths are not known, we could not determine the relative contribution of each process for various lines from our experimental data. The asymmetric shape of the 0.899-μ ($R_1 \rightarrow Z_4$) line indicates that the resonant one-phonon emissions from the Z_4 level gives a dominant contribution to the width. An analysis of this line shape using Eq. (2) of Ref. 4 showed that the direct $Z_4 \rightarrow Z_3$ and Z_2 processes have major effects on the shape and width of this line.

Since the lifetime broadenings of the R_1 levels are completely negligible, a low-temperature linewidth $\sim 0.6\ \text{cm}^{-1}$ for the $Z_1 \rightarrow R_1$ transition of YAlG:Nd is ascribed to the inhomogeneous strain broadening. The fact that the residual width for the $R_1 \rightarrow Y_1$ transition

is almost the same suggests that the probabilities of the $Y_1 \rightarrow Z$ multiphonon emissions are not large enough to affect the linewidths. The broader residual width of the $Z_1 \rightarrow R_2$ (or $R_2 \rightarrow Y_1$) transition compared with that of the $Z_1 \rightarrow R_1$ (or $R_1 \rightarrow Y_1$) transition can be explained either by the direct $R_2 \rightarrow R_1$ transition or different magnitude of the strain broadenings. Examination of all the $R \rightarrow Y$, Z transitions in YAlG:Nd at 77°K shows that the width of the transition from the R_2 level is not always bigger than that of corresponding transition from the R_1 level. This fact, in addition to the observation of slight increase of the R-level splitting with temperature, strongly supports the latter interpretation. The effect of the static crystal strains on the linewidths will be discussed later. In Fig. 6, the residual widths ~ 4 cm^{-1} of the $Z_1 \rightarrow R_1$, and $R_1 \rightarrow Y_1$ transitions are ascribed again to the inhomogeneous strain broadening. The broader width of the $Z_1 \rightarrow R_2$ transition is due to the $R_2 \rightarrow R_1$ resonant phonon emission, or due to the different contribution of the strain effect.

V. DISCUSSION

It may be possible to derive a gross feature of the effective phonon-density spectrum from vibronic sidebands of no-phonon lines. The weak satellite emission lines observed in YAlG:Nd at low temperatures were very narrow, for example, the 1.066- and 0.876-μ lines were ~ 1.3 cm^{-1} and ~ 1.9 cm^{-1} wide, respectively, at 77°K. These satellites do not seem to reflect the crystal-phonon spectrum. On the contrary, the fluorescence spectrum of the Stokes sideband of the R lines in YAlG:Cr is very similar to the phonon-density spectrum of YAlG,[18] and this intense emission sideband is mainly attributable to the R transition associated with emission of one quantum of lattice vibrational energy. The difference of the intensities of the vibronic sidebands for the Nd^{3+} and Cr^{3+} ions in YAlG may indicate the different magnitudes of the orbit-lattice couplings for these two ions. This sort of difference in coupling strength between rare-earth and transition-metal ions has also been observed in multiphonon relaxation rates.[19]

Burns *et al.*[17] measured the temperature dependence of the positions and widths of the R lines of the Cr^{3+} ion in several garnets. The fitting with Eq. (3) of the $E(T)$-versus-T curve for YAlG:Cr required Θ_D of 560°K. That this value is close to $\Theta_D \sim 600$°K for YAlG:Nd may indicate that the effectively coupled phonon spectra are not very different for the Cr^{3+} and Ne^{3+} ions.

An attempt was made to estimate the effective Debye temperature for YAlG from the phonon-assisted flourescent spectrum. If $\rho(\omega)$ is the effective density of the phonons which interact with the impurity, the Raman-type linewidths and shifts may be expressed as follows:

$$E^R(T) \propto \int_0^\infty \rho(\omega) n(\omega) d\omega , \tag{4}$$

$$\Gamma^R(T) \propto \int_0^\infty [\rho(\omega)]^2 n(\omega)[n(\omega)+1] d\omega . \tag{5}$$

These Raman terms were calculated for several temperatures, with $\rho(\omega)$ deduced from the Stokes emission sidebands of the R lines in YAlG:Cr. The relation[20]

$$I(\omega) \propto [n(\omega)+1]\rho(\omega)/\omega^2 \tag{6}$$

was assumed, where $I(\omega)$ is the intensity of the vibronic sidebands and $\hbar\omega$ is the energy measured from the no-phonon line. By comparing the calculated temperature dependence with Eqs. (2) and (3), effective Debye temperatures of about 900 and 750°K were obtained for the thermal shift and broadening, respectively. Although these values are considerably larger than the measured ones, this result agrees with experiment in that the characteristic temperature to explain the thermal shift is 20% higher than for the linewidth. The relatively big discrepancy between the thus estimated Θ_D's and the observed values may result from a considerable contribution of many-phonon processes to vibronic sidebands and/or from an inadequacy of the very simple relation (6) as a basis for deducing the effective phonon-density spectrum of YAlG:Nd from the data on YAlG:Cr.

Most of the spectral lines examined shifted to the longer wavelengths when the crystal temperature was increased and this red shift fitted well with the Raman-shift term of the theory. These facts suggest that all the energy levels examined move downwards with increasing temperature and that the shifts caused by thermal lattice expansion are negligible. The observed blue shifts of the $R \rightarrow Z_5$ and $R \rightarrow Y_6$ transitions in YAlG:Nd should be explained by exceptionally fast lowerings of the terminal states of the fluorescence (Z_5, Z_6).

It seems unlikely that the Raman-shift coefficients α_1's are unusually large in the Z_5 and Y_6 states. Further, as shown by the following discussions, the effect of resonant one-phonon emissions such as the $Z_5 \rightarrow Z_4$ transition is considered to give shifts opposite to the observation. With the Debye-model phonons, two states whose energy separation is smaller than $k\Theta_D$ attract each other at high temperatures and repel at low temperatures by the effect of the $E_1^D(T)$ term. Calculation shows that the attraction occurs when T is higher than $\Theta_D/5$ and $\Theta_D/10$ for $|E_j - E_i| = k\Theta_D/2$ and $= k\Theta_D/4$, respectively. In case of the $Z_5 \rightarrow Z_4$,

[18] J. P. Hurrell, S. P. S. Porto, I. F. Chang, and S. S. Mitra, Phys. Rev. **173**, 851 (1968).

[19] L. A. Riseberg, H. W. Moos, and W. D. Parthlow, IEEE J. Quantum Electron. **QE-4**, 609 (1968).

[20] A. A. Maradudin, in *Solid State Physcis*, edited by F. Seitz and D. Turnbull (Academic Press Inc., New York, 1966), Vol. 18, p. 273.

TABLE I. Comparison of typical linewidths of the Nd^{3+} ions in several host crystals at room temperature. In the fourth and fifth columns, the relative values of effective Debye temperature estimated from the linewidth data are compared with those of the cutoff energy of the coupled phonon.

Host crystal	Cutoff energy of coupled phonon	Typical width and wavelength of Nd lines at room temperature		Relative value of estimated Θ_D	Relative value of phonon cutoff energy
$LaBr_3$	175 cm^{-1} [a]	~17 cm^{-1}	1.068 μ	1.0	1.0
$LaCl_3$	260 cm^{-1} [a]	~11 cm^{-1}	1.064 μ	1.3	1.5
LaF_3	350 cm^{-1} [a]	~24 cm^{-1}	1.063 μ [b]	2.1	2.0
Y_2O_3	550 cm^{-1} [a]	~12 cm^{-1}	1.073 μ [b]	2.7	3.1
YAlG	~800 cm^{-1}	~4 cm^{-1}	1.0615 μ	4.1	4.6

[a] L. A. Riseberg and H. W. Moos, Phys. Rev. **174**, 429 (1968).
[b] W. W. Holloway, Jr., M. Kestigian, F. F. Y. Wang, and G. F. Sullivan, J. Opt. Soc. Am. **56**, 1409 (1966).

Z_3, $\cdots$ direct processes in YAlG:Nd, repulsion is expected in the temperature ranges of interest, since the energy separation is bigger than the main energy region of the effective phonon density. This should reduce the lowering rate of the Z_5 state, and therefore does not explain the observed blue shift.

For $|E_i-E_j|>k\Theta_D$, repulsion of the two states results from the interaction via H.[1] The case where the energy separation is much greater than the phonon cutoff energy is included in the Raman term $E_1{}^R(T)$. On the other hand, when the energy separation is a little bigger than the phonon cutoff energy, the magnitude of the repulsion is considerable and depends strongly on the energy separation. Since other causes do not seem to explain the blue shift, we tentatively ascribe this to the pushing effect of nearby higher-lying manifolds ($^4I_{11/2}$,$^4I_{13/2}$). That the blue shifts are observed only for the transitions to the uppermost levels of manifolds and that thermal shifts are small for the $R\rightarrow Y_5$ line in YAlG:Nd and $R_1\rightarrow Y_6$ line in FAP:Nd are consistent with this interpretation.

Now, we shall consider the effect of static crystal strains on the spectral linewidths. In the crystal-field approximation, the effect of the electric field produced by surrounding ions on the energies of the impurity levels may be expressed by use of several crystal-field parameters $V_n{}^m=A_n{}^m\langle r^n\rangle$.[21] In case of the $^4F_{3/2}$ state of the Nd^{3+} ion in YAlG, the crystal-field energies are calculated by using the operator-equivalent method[22] as

$$E_{R_2}=3\alpha_J[(V_2{}^0)^2+(V_2{}^2/\sqrt{3})^2]^{1/2},$$
$$E_{R_1}=-3\alpha_J[(V_2{}^0)^2+(V_2{}^2/\sqrt{3})^2]^{1/2}, \quad (7)$$

where α_J is the second-degree multiplicative factor, and $V_2{}^0$ and $V_2{}^2$ are the second-degree crystal-field parameters. The multiplicative factors have been calculated for many J manifolds of the Nd^{3+} ion by using Wybourne's wave functions.[16]

Since α_J for the $^4F_{3/2}$ manifold is positive, when the absolute value of $V_2{}^0$ (or $V_2{}^2$) increases because of static crystal strains, the energy of the R_2 level increases while that of the R_1 level decreases. On account of the spacial variation of the crystal strains, inhomogeneous width of the $R_2\leftrightarrow\Omega$ line should be broader or narrower than that of $R_1\leftrightarrow\Omega$ line according as the state Ω moves downwards or upwards when $|V_2{}^0|$ (or $|V_2{}^2|$) is increased. The fact that the low-temperature width of the $R_2\rightarrow Y_i$ line is broader than the $R_1\rightarrow Y_i$ line only for $i=1$, 5, and 6 in YAlG:Nd is thus explained very well. In other words, this experimental observation indicates that the fluctuation of the second-degree crystal-field parameters $V_2{}^0$ and/or $V_2{}^2$ makes an important contribution to the inhomogeneous broadenings of the spectral lines in YAlG:Nd. In garnets, the values of the second-degree crystal-field parameters are extremely sensitive to the exact position of the impurity ion, and accordingly to the crystal strains.[23] This fact is consistent with the above statement. The differences of the low-temperature linewidths between the $R_2\rightarrow Y_i$ and $R_1\rightarrow Y_i$ transitions in YAlG:Nd were less than 1 cm^{-1}, and the average ~0.4 cm^{-1} agreed with the difference between the residual widths of the $Z_1\rightarrow R_2$ and $Z_1\rightarrow R_1$ transitions. From this result, the fluctuation in the average value of $V_2{}^0$ and/or $V_2{}^2$ is estimated to be at least $\pm 0.2\%$.

VI. LINEWIDTHS IN DIFFERENT HOST MATERIALS

Among factors contributing to the linewidths, statistical broadening is related to the homogeneity of the crystalline field that each ion sees and is usually large in case charge compensation is necessary. The relatively broad residual widths of the spectral lines in FAP:Nd may be due in part to the charge compensation and to the large crystal-field parameters.

As to the direct and Raman widths, it is concluded from Eq. (2) that narrow lines are expected not only for weak impurity-phonon coupling but also for host crystals with high sound velocity or with high Debye temperature. Typical widths of Nd lines in several host materials at room temperature are compared in Table I. There seems to be a tendency for the linewidth to decrease as the crystal phonon cutoff frequency increases. The irregularity seen in the linewidth data is

[21] See, for example, M. T. Hutchings, in *Solid State Physics*, edited by F. Seitz and D. Turnbull (Academic Press Inc., New York, 1964), Vol. 16, p. 227.
[22] K. W. H. Stevens, Proc. Phys. Soc. (London) **A65**, 209 (1952).
[23] M. T. Hutchings and W. P. Wolf, J. Chem. Phys. **41**, 617 (1964).

considered to be mainly due to the difference of the coupling strengths. This may be verified by the fact that the reported ratios $\gamma=W_n/W_{n-1}$ of the spontaneous n-phonon relaxation rate to the $(n-1)$-phonon relaxation rate in rare-earth ions are very different between $LaBr_3$, and $LaCl_3$ ($\gamma=0.037$) host crystals on the one hand, and LaF_3 ($\gamma=0.14$) and Y_2O_3 ($\gamma=0.12$) host crystals on the other hand.

In a very simple model, this ratio may be expressed as follows[24]:

$$\gamma=b\frac{C^2}{\langle\Delta E^2\rangle}\frac{\hbar N^{5/3}}{\omega_m\rho_m}, \tag{8}$$

where $1/\langle\Delta E^2\rangle$ is a suitable average of the inverse square of intermediate-state energies, ω_m is the highest angular frequency of coupled phonons, ρ_m is mass density of the crystal, N is the number of atoms in unit volume, and b is a numerical constant. With $\Theta_D=(\hbar v/\kappa)(6\pi^2N)^{1/3}$ and $\xi_6(\Theta_D/T)\propto(\Theta_D/T)^5$ at high temperatures such as 300°K, we obtain the dependence of the Raman widths at a given temperature on γ, ω_m, and Θ_D as

$$\Gamma^R\propto\gamma^2\omega_m{}^2/\Theta_D{}^5. \tag{9}$$

The ratios of Θ_D's estimated using this relation are compared with those of the ω_m's in the fourth and fifth columns of Table I. In the estimation, we assumed that the linewidths at room temperatures may be ascribed to Γ^R, except in YAlG, where the strain width is known. We further assumed that $1/\langle\Delta E^2\rangle$ is the same for different host crystals and used $\gamma=0.12$ for YAlG. The result seems to be very reasonable and gives support to the above statement that the phonon-induced linewidths are closely related to the phonon-impurity coupling strength and phonon distribution of host materials.

When the terminal state of the laser transition is located much higher above the ground state compared with kT, as in the well-known 1.06-μ laser line of the Nd^{3+} ion, the threshold pumping power for laser oscillation is directly proportional to the width of the laser line. Therefore, it is very important that the laser line has narrow width at the operating temperature. From the above consideration, it is predicted that crystals with high Debye temperature and with weak phonon-impurity coupling are suitable, especially at high temperatures, for laser host materials. In case of the 1.06-μ lines of Nd^{3+}, the suitability of host crystals with high phonon cutoff energies is predicted also from the standpoint of multiphonon relaxations.[19] These predictions seem to be verified by the comparison of laser thresholds in several crystals doped with the Nd^{3+} ions (Table II).

YAlG and FAP are hard crystals with high phonon cutoff energies. Furthermore, as shown by the very weak intensity of vibronic sidebands, the rare-earth–phonon interactions in these crystals are considered to be relatively weak.[25] Therefore, it is understandable that these crystals show narrow spectral lines and are very good host materials for lasers.

TABLE II. Comparison of threshold pumping energies for laser oscillation at room temperature in several crystals doped with the Nd^{3+} ions.

Host crystal	Crystal Debye temperature[a] (°K)	Threshold pumping energy for laser oscillation[b] (J)
KI	132	210
NaI	164	195
KBr	174	210
KCl	235	200
NaCl	321	175
CaF_2	510	30
LiF	732	2

[a] From *American Institute of Physics Handbook* (McGraw-Hill Book Co., New York, 1957).
[b] From the data of R. C. Vickery, in *Proceedings of the Third International Congress on Quantum Electronics*, edited by P. Grivit and N. Bloembergan (Columbia University Press, New York, 1964), p. 861.

ACKNOWLEDGMENTS

The author wishes to thank J. E. Geusic for many stimulating discussions and for a critical reading of the manuscript. He is indebted to L. G. Van Uitert for providing samples, to H. M. Macros for technical assistance, and to T. C. Rich for computer calculations. He is also grateful to L. A. Riseberg and co-workers for sending a report of their results on multiphonon relaxations, which proved very helpful.

[24] A. Kiel, in *Proceedings of the Third International Congress on Quantum Electronics*, edited by P. Grivit and N. Bloembergan (Columbia University Press, New York, 1964), p. 765.

[25] L. A. Riseberg and H. W. Moos, Phys. Rev. 174, 429 (1968).